Questions arising for future surface diffusion studies using scattering techniques—the case of benzene diffusion on graphite basal plane surfaces

2010 J. Phys.: Condens. Matter 22 304014

(http://iopscience.iop.org/0953-8984/22/30/304014)

IOP Publishing Journal of Physics: Condensed Matter

J. Phys.: Condens. Matter **22** (2010) 304014 (12pp) doi:10.1088/0953-8984/22/30/304014

Questions arising for future surface diffusion studies using scattering techniques—the case of benzene diffusion on graphite basal plane surfaces

Irene Calvo-Almazán, Tilo Seydel and Peter Fouquet[1]

Institut Laue Langevin, BP 156, F-38042 Grenoble Cedex 9, France

E-mail: fouquet@ill.eu

Received 27 February 2010, in final form 3 May 2010
Published 13 July 2010
Online at stacks.iop.org/JPhysCM/22/304014

Abstract

This paper gives a review of recent work on benzene diffusion on graphitic carbon surfaces using neutron and helium scattering spectroscopy as well as computational modelling. Recent spin-echo spectroscopy measurements have demonstrated that benzene/graphite displays almost perfect Brownian diffusion and that it can be used as a tool to study dynamic friction. Incoherent neutron backscattering measurements, on the other hand, reveal a jump diffusion behaviour, related to the molecular rotational modes of the benzene rings. Molecular dynamics (MD) simulations have delivered a very detailed picture of the adsorbate dynamics. We use this review to illustrate the open questions and possible future directions of this research field.

(Some figures in this article are in colour only in the electronic version)

1. Introduction

The technical possibilities for experimental studies of surface diffusion and friction have been expanded dramatically in the last ten years, both in spectroscopy [1–8] and in scanning microscopy [9–20]. The new research tools are giving us new insights into the microscopic world and raise a large portfolio of fascinating scientific questions. In this article we will explore some of the topics that have arisen, concentrating on spectroscopic helium and neutron scattering techniques and their theoretical modelling.

A particularly interesting field of study is the diffusion and friction of aromatic hydrocarbon molecules or graphene adsorbed on graphite surfaces. The aim of these studies is to reveal the mechanism of friction (reduction) by graphite and to help lay the mechanical basis for carbon based nanomachines. Recent helium and neutron spin-echo measurements have been used to show that diffusion in this system is almost independent of the shape of the potential energy surface (PES) and that dynamics are dominated by a dynamic friction term [8, 21]. The measurements can, thus, provide a link between the molecules' diffusion and friction. Molecular dynamics calculations are able to model the measured data with surprising accuracy, allowing—in theory—to produce a very detailed picture of the diffusion and friction in this case down to the atomic level [21]. There are, however, many open questions, such as the coupling between translational and rotational degrees of freedom. This paper will make a résumé of the possible future directions of research and will show data that hint on the phenomena to be observed.

The diffusion of atoms and molecules on surfaces is both a scientifically and technically important subject of study [22–25]. Over macroscopic length scales diffusion generally follows—with some notable exceptions—Fick's laws of diffusion. However, on the length scale of atoms or molecules, the discrete nature of matter leads to more complex forms of motion. On the one hand this complicates the description and understanding of the observed motion, but on the other hand this should allow finding ways of controlling and manipulating motion in the future. The experimental study of diffusion requires techniques that trace the motion of atoms on sub-nanometre length scale. For temperatures above about 50 K, it will normally be necessary that the time resolution of the techniques of choice is in

[1] Author to whom any correspondence should be addressed.

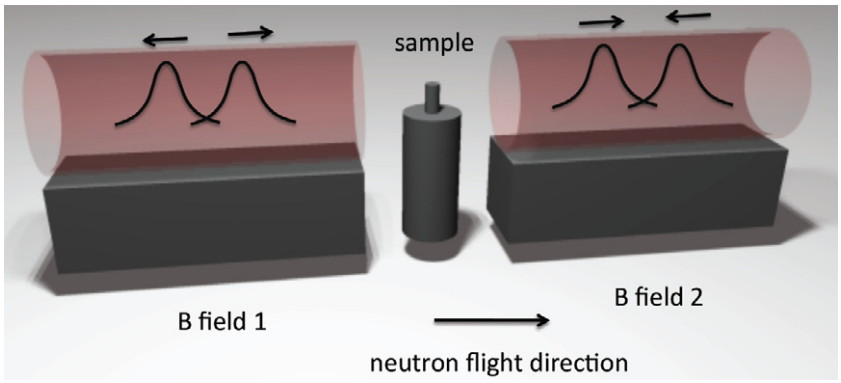

Figure 1. Illustration of the measurement principle of NSE spectroscopy in the quantum mechanical picture: the wavefunction of the (spin polarized) neutron is split into two part wavefunctions in B field 1 which are accelerated and decelerated, respectively. After scattering from the sample with a relative time delay, t, the two part wavefunctions are recombined by a field with an equal, but opposite strength.

the pico- to nanosecond range. This domain is the field of excellence of quasielastic neutron scattering (QENS) and helium atom scattering (QHAS). The potential of QENS and QHAS for investigations of surface diffusion has been demonstrated in several recent studies [4, 5, 8, 21]. Two recent instrumental developments, in particular, have allowed for a growing number of surface diffusion studies using quasielastic scattering techniques. On the neutron side, large signal gains have been and will be achieved by using larger detectors and better neutron delivery systems [26–28], and on the helium atom scattering side, the realization of helium spin-echo spectrometers has pushed the limits of the technique into the range of diffusion studies [5, 29].

The usefulness of dynamical data that are collected from scattering experiments is strongly dependent on the quality of the theoretical framework available, as scattering experiments only give information about a statistical ensemble, rather than specific atoms. For surface diffusion studies a solid theoretical framework exists both in terms of molecular dynamics simulations and more generic models. However, a large number of theoretical models can only now be tested using the newly available quasielastic scattering techniques.

This paper is organized as follows: we commence with a description of the technical aspects of the presented research. We briefly explain spin-echo and backscattering spectroscopy and we include a short description of the graphite samples and the benzene monolayer structure. Section 4 summarizes the theoretical framework for diffusion studies. In the following sections we give an overview of recent experimental results and the progress in computational modelling. The paper closes with a summary of our present understanding and an outline of the future perspectives for experimental and theoretical studies of aromatic hydrocarbon diffusion on carbon surfaces.

2. Methods

The measurements that are shown in the following sections have been performed on the neutron spin-echo (NSE) spectrometer IN11 and the high-resolution neutron backscattering (BS) spectrometer IN16, both situated at the Institut Laue-Langevin, Grenoble, France [30].

The NSE measurement [4, 31] is a correlation measurement, which compares two snapshots of the sample that are separated by a time, t. A quantum mechanical description of NSE spectroscopy [32] illustrates the origin of the correlation measurement (see figure 1): a thermal beam of neutrons is first spin polarized and then exposed to a magnetic field that is perpendicular to the neutron polarization vector. Due to the applied magnetic field, the neutron wavepackets are split into two part wavepackets, one of which is accelerated while the other is decelerated. The two part wavepackets, therefore, arrive at the sample with a time lag, t. If the atoms in the sample have moved within the time window of the measurement, then the neutrons will see them at different atomic positions. After scattering, the outgoing wavepackets are exposed to an identical magnetic field of the opposite direction, such that the separate wavepacket components are recombined before entering a polarization (coherence) analyser and the detector. If the two wavepackets scatter identically, i.e., there has been no atomic motion in the sample, there is no loss in the beam averaged polarization. However, changes in the atomic positions during the time window, t, lead to a loss in coherence between the two part wavepackets, giving a subsequent loss in polarization and a decrease in the corresponding intermediate scattering function, $I(\mathbf{Q}, t)$. The time lag, t, is known as the *spin-echo* time and is given by

$$t = \left(\gamma \int B \cdot \mathrm{d}l\right) \frac{m^2}{2\pi h^2} \lambda^3, \tag{1}$$

where γ and m are the gyromagnetic ratio and mass of the neutron, respectively, $\int B \cdot \mathrm{d}l$ is the magnetic field line-integrated over the length of the neutron paths in the magnetic fields and averaged over the range of possible neutron trajectories, and λ is the neutron wavelength. A rough energy monochromatization of about 20% $\Delta\lambda/\lambda$ is sufficient for NSE spectroscopy, since NSE measures energy differences rather than energies of neutrons. This monochromatization is typically achieved by a mechanical velocity selector.

We would like to stress that in contrast to other neutron spectroscopy techniques, an NSE experiment provides the real part of the normalized intermediate scattering function $I(\mathbf{Q}, t)$,

rather than the dynamic scattering function $S(\mathbf{Q}, \omega)$ [31]. Here, $\hbar\mathbf{Q}$ is the momentum transfer, $\hbar\omega$ is the energy transfer at the sample and t is the time. The intermediate scattering function is the time-energy Fourier transform of the dynamic structure factor, $S(\mathbf{Q}, \omega)$:

$$\frac{\Re[I(\mathbf{Q}, t)]}{I(\mathbf{Q}, 0)} = \frac{\int S(\mathbf{Q}, \omega)\cos(\omega t)\,\mathrm{d}\omega}{\int S(\mathbf{Q}, \omega)\,\mathrm{d}\omega}. \tag{2}$$

$I(\mathbf{Q}, t)$ is the spatial Fourier transform of the Van Hove pair correlation function, $G(\mathbf{r}, t)$, which provides a statistical description of the motion of the species from which the neutrons scatter [33] and can be interpreted classically as the probability of finding a scatterer at $(\mathbf{r}' + \mathbf{r}, t' + t)$ given there was a scatterer at $(\mathbf{r}', t')$, averaged over all $\mathbf{r}'$.

HeSE spectroscopy follows the same theoretical framework as the one established for NSE, except that the neutron probe particles are replaced with neutral—and surface sensitive—helium atoms [4]. Whereas neutron scattering can be either predominantly coherent or incoherent, helium scattering is always coherent, as the interaction is mediated by the valence electrons.

Backscattering spectroscopy (BS) is an inverse geometry spectroscopic technique that measures the dynamic scattering function, $S(\mathbf{Q}, \omega)$, with a very high energy resolution in the sub-μeV regime [34, 35]. At IN16 a wavelength band is extracted from the neutron guide by a double deflecting crystal set-up and subsequently monochromatized using a single crystal in backscattering (Bragg angle $\theta = 90°$) [30]. After scattering from the sample, the neutrons are back-reflected from analyzing monochromators onto the detectors, allowing only elastically scattered neutrons to be detected ($E_\mathrm{i} = E_\mathrm{f}$, where E_i and E_f are the kinetic energies of the incoming and scattered neutrons, respectively). The energy window for this so-called 'fixed window scan' is determined by the quality of the monochromator crystals (≈0.9 μeV for the measurements shown below). Quasi- and inelastic spectra can be recorded by moving the backscattering monochromator parallel to the incoming beam on a so-called Doppler drive. IN16 can reach a dynamic window of −15 to 15 μeV.

For all experiments shown below we adsorbed benzene molecules from the gas phase at liquid nitrogen temperature. Coverages were verified by measuring adsorption isotherms using a high-resolution absolute pressure meter.

The substrates were Papyex exfoliated graphite (Papyex Grade N998, Carbone Lorraine, Gennevilliers, France) with a specific surface area of 23 $\mathrm{m}^2\,\mathrm{g}^{-1}$ and Vulcan XC-72 as well as BP2000 carbon blacks (both from Cabot Corporation, Boston, USA) with specific surface areas of 250 $\mathrm{m}^2\,\mathrm{g}^{-1}$ and 1690 $\mathrm{m}^2\,\mathrm{g}^{-1}$, respectively. The specific surface areas were determined by BET adsorption isotherms. Hydrogenated benzene molecules (*h-benzene*, >99.9%, Sigma-Aldrich Chimie, St Quentin Fallavier, France) and fully deuterated benzene (*d-benzene*, 99.6% D, CEN Saclay, Gif-Sur-Yvette, France) were employed in the experiments, as indicated in the experimental sections, leading to mainly incoherent and coherent scattering in the experiments, respectively.

According to low energy electron diffraction (LEED) [36] and x-ray diffraction [37] measurements the benzene molecules are adsorbed flat on the surface at the temperatures and surface coverages at which the present measurements were conducted. The super-structure of a full monolayer (ML) of benzene on basal plane graphite is $(\sqrt{7} \times \sqrt{7})$R19.1°.

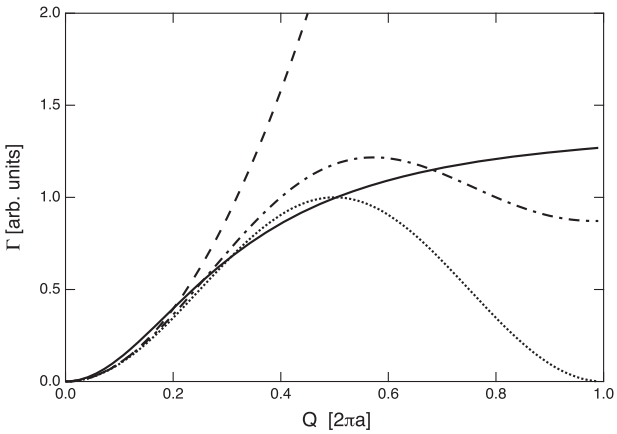

Figure 2. Theoretical Γ versus Q graphs arising from the Brownian (dashed line), Chudley–Elliott (dotted line), isotropic Chudley–Elliott (dashed–dotted line) and Singwi–Sjolander (continuous line) diffusion models. The x axis is scaled such that a corresponds to the distance between two neighbouring minima in the potential energy surface.

3. Theoretical models for molecule diffusion

The spectroscopic scattering methods discussed in this article will show diffusion processes, generally, as either a Lorentzian *quasielastic* broadening of the elastic peak ($S(Q, \omega)$) or an exponential decay of the dynamic signal ($I(Q, t)$). The broadening, Γ, of the elastic peak is linked to the decay constant, τ, of the intermediate scattering function by the equation (Fourier transform pair)

$$\Gamma(Q) = \frac{\hbar}{\tau}. \tag{3}$$

It is very useful for understanding molecular diffusion processes to classify the diffusion behaviour according to a set of basic theoretical models [34, 38]. We can, for example, distinguish between almost free *ballistic* motion or a *jump* motion, where the molecules stay at given positions until they jump, eventually, to a neighbouring site. For many idealized diffusion processes it is possible to calculate the behaviour of the quasielastic broadening as a function of the momentum transfer. The result of these considerations is a set of Γ–Q profiles which are characteristic for certain diffusion behaviours (figure 2). Below, we list the most important models. These models have been developed for the simple case of single particle or self diffusion and are only strictly valid for describing incoherent scattering measurements. Under certain conditions, such as e.g. negligible coverage dependence of diffusion data, they can be applied to coherent scattering measurements as well [39].

In *ballistic diffusion* the molecules move in straight lines with negligible surface interaction until they hit another

molecule or a defect. This diffusion process represents a two dimensional ideal gas and is characterized by a linear dependence of Γ on Q [40, 41]:

$$\Gamma \propto Q. \tag{4}$$

Note that in this case the quasielastic broadening has a Gaussian functional form in contrast to all other cases, mentioned below.

The *Brownian diffusion model* [34] describes a continuous motion which is characterized by a square law dependence of Γ on the momentum transfer Q:

$$\Gamma(Q) = \hbar D Q^2. \tag{5}$$

Here, D stands for the Fick diffusion constant, which is given by the Einstein expression [42]:

$$D = \frac{k_B T}{m\eta}, \tag{6}$$

where η is the friction parameter, and m is the mass of the diffusing molecules.

The *Chudley–Elliott model* [34, 43] describes a jump motion, where the molecules are considered to be stationary for a given time, after which they jump to the nearest trough in the potential energy surface. In this model, the dependence of Γ on the momentum transfer Q follows:

$$\Gamma(Q) = \hbar \frac{4}{n\tau_{CE}} \sum_j \sin^2\left[\frac{\vec{Q}\cdot\vec{j}}{2}\right], \tag{7}$$

where τ_{CE} is the *residence time*, which is the average time interval spent by a particle at a certain equilibrium position. It also gives account of the probability of an atom 'jumping' from one equilibrium position (energy minimum in the PES) to another, both of them linked by the *jump vector* $\vec{j}$. τ_{CE} is assumed to be the same for all the sites. The summation in equation (7) runs over all n neighbouring sites.

The *isotropic Chudley–Elliott model* [34] is a derivation of the Chudley–Elliott model, which arises from the average of the momentum transfer Q over all possible directions of the scattering vector in equation (7). Thus, the dependence of the quasielastic broadening on the momentum transfer can be written:

$$\Gamma(Q) = \frac{2\hbar}{\tau_{CE}}\left[1 - \frac{\sin(Qa)}{Qa}\right]. \tag{8}$$

The *Singwi–Sjolander model* [34, 44] is a synthesis of the Brownian and the Chudley–Elliott model. The main hypothesis is that particles execute an oscillatory motion for a mean time interval τ_o, and then diffuse for a mean time interval τ_l. If τ_o is taken to be greater than τ_l ($\tau_o \gg \tau_l$), then the quasielastic broadening depends on the momentum transfer Q as follows:

$$\Gamma(Q) = \frac{2\hbar}{\tau_o}\left[1 - \frac{\exp(-2W)}{1 + Q^2 D\tau_o}\right], \tag{9}$$

where D is the *effective diffusion coefficient* and W is the Debye–Waller factor. D depends on the two possible states of the particle: oscillation and diffusion. Its definition is:

$$D = \frac{\langle R^2\rangle + \langle l^2\rangle}{6(\tau_o + \tau_l)}. \tag{10}$$

Here, $\langle R^2\rangle$ is the mean square radius of the thermal cloud due to the oscillations of the particle at a certain temperature, and $\langle l^2\rangle$ is the square mean free path for the diffusive motion of the particle. Assuming that $\langle l^2\rangle \gg \langle R^2\rangle$, equation (10) can be written:

$$D_l\tau_l \approx D\tau_o\left(1 + \frac{\tau_l}{\tau_o}\right). \tag{11}$$

Depending on the ratio $\frac{\tau_l}{\tau_o}$ the model tends to approach either the Brownian diffusion ($\tau_l \gg \tau_o$) or the jump diffusion model ($\tau_l \ll \tau_o$). Finally, W is the Debye–Waller factor which gives account of the effect of temperature on the behaviour of the particles. In this case, it describes the oscillations of the molecules around the equilibrium position, and it is given by:

$$2W = \tfrac{1}{2}\langle R^2\rangle Q^2. \tag{12}$$

We would like to stress that the Chudley–Elliott and Singwi–Sjolander models contain the Brownian diffusion as a long range diffusion limit, i.e., the curvature of the Γ/Q behaviour converges to a parabola for $Q \to 0$.

4. Long range diffusion of benzene on basal plane graphite: coherent scattering neutron and helium spin-echo studies

Neutron and helium spin-echo measurements of benzene diffusion on basal plane graphite surfaces have been described in detail in recent studies [8], and here we only include the results in a summary form for completeness. Most importantly these studies demonstrate the feasibility of combined helium and neutron spectroscopy measurements of polycyclic hydrocarbon molecules on graphite surfaces and show excellent agreement of the results of these two spectroscopy techniques. Hence, the two techniques can be used in a complementary fashion: helium atom scattering has a substantially higher surface sensitivity and a high cross section for scattering from adsorbate molecules (van der Waals interaction between helium atoms and surface molecules); neutron scattering on the contrary can obtain signals from molecules adsorbed in confinement and picks up rotational motion much better (scattering from the nuclei of the sample atoms).

The diffusion of benzene on a graphite substrate was measured for sub-monolayer coverages in the 1.5–150 K temperature range, using both NSE and HeSE [8, 45]. In these experiments different graphite substrates were used for NSE and HeSE, respectively, that are well adapted for both neutron scattering (exfoliated graphite) and helium scattering studies (highly oriented pyrolytic graphite, HOPG). Deuterated benzene (C_6D_6) was used in the NSE experiments and hydrogenated benzene (C_6H_6) was used in the HeSE experiments, leading to predominantly coherent scattering in both cases. The results demonstrate a regime of continuous random motion and have provided the first definitive surface observation of a Brownian, high friction regime on the atomic scale. For the first time it was possible to determine the *dynamic* friction coefficient on a molecular level with a reasonable precision ($\eta = 2.2 \pm 0.1$ ps^{-1}) [8]. We

note that the theoretical framework of the analysis was based on the incoherent scattering theory described above, although coherent scattering was used. This is important as, generally, incoherent scattering obtains the self diffusion coefficient, D_s, which is needed for the determination of the friction coefficient, whereas coherent scattering leads to the chemical diffusion coefficient, D_c. These are not necessarily equal, and a careful analysis was used to obtain D_s and the friction coefficient of a freely moving particle. Most importantly, it was shown that D_c has a negligible coverage dependence (negligible inter-adsorbate interactions) [46] and that no correlation effects appear in the data. Langevin molecular dynamics calculations were used to recover D_s.

The evaluation of the spectra at different temperatures allowed an activation energy E_a to be obtained via the Arrhenius law:

$$\Gamma = h\nu \exp\left[-\frac{E_a}{k_B T}\right], \tag{13}$$

where ν is the attempt frequency for diffusional jumps and k_B is the Boltzmann constant. The NSE and HeSE data gave a value of $E_a = 17 \pm 12$ meV, consistent with a lateral potential energy surface whose corrugation is small enough to play a negligible role in the motion at the temperature of the experiments ($k_B T = 12$ meV at 140 K) [8]. Corresponding force-field molecular dynamics calculations also indicated Brownian diffusion and a low lateral diffusion barrier of 11 ± 2 meV, in agreement with the experimental data [21].

5. Self diffusion of benzene on basal plane graphite: incoherent neutron backscattering study

The coherent spin-echo measurements described above were able to disclose the translational self diffusion coefficient and proved that no correlation effects appear up to momentum transfers of 1.5 Å^{-1}. Although, it would now be desirable to study the *incoherent* scattering directly. Neutron backscattering or time-of-flight spectroscopy can be used to study the *self diffusion* of the molecules by using hydrogen terminated benzene, C_6H_6, as an adsorbate on basal plane graphite. The feasibility of such an approach was investigated in an exploratory measurement on the BS spectrometer IN16 at ILL on 1 ML of h-benzene adsorbed on an exfoliated graphite substrate.

The presence of hydrogen atoms in the h-benzene molecules gives rise to strong incoherent scattering, which is ideal for a high signal in neutron time-of-flight spectrometers [34, 38]. In fact, the neutron incoherent scattering cross section, σ_{inc}, of hydrogen is more than 10 times as large as the coherent scattering cross section, σ_{coh}, of either deuterium or carbon ($\sigma_{inc}(H) = 80.3$ barn, $\sigma_{coh}(H) = 1.8$ barn, $\sigma_{coh}(D) = 5.6$ barn, and $\sigma_{coh}(C) = 5.6$ barn). We would like to note here that for spin-echo spectroscopy it is preferable to use deuterated molecules, as incoherent scattering leads to a depolarization of a spin polarized neutron beam and, therefore, to a strong decrease of the signal-to-noise ratio in NSE spectroscopy.

Table 1. Values of the fitting parameters at different temperatures for the Chudley–Elliott model (equation (7)).

T (K)	τ_{CE} (10^{-9} s)	a (Å)
80	1.8 ± 0.3	2.2 ± 0.2
90	2.1 ± 0.1	2.1 ± 0.1
100	1.77 ± 0.07	2.1 ± 0.1
110	1.56 ± 0.03	2.08 ± 0.04
120	1.21 ± 0.03	2.00 ± 0.06

The experiments were carried out at temperatures in the range: 10 K $< T <$ 120 K and in the momentum transfer range: 0.4 Å^{-1} $< Q <$ 1.7 Å^{-1}. The fitting of the quasielastic peak of the scattering function $S_{inc}(Q, \omega)$ assumed a summation of a pure Gaussian function for the elastic part (equal to the instrumental resolution function) and a Voigt profile for the energy-broadened signal (see figure 3). The quasielastic broadening Γ is defined as the HWHM of the Lorentzian part of the Voigt profile. Figure 3 displays a representative set of fitted spectra. The chosen theoretical function gives a good fit to the experimental scattering functions, which demonstrates that a single Voigt function is sufficient to describe the quasielastic component of the measured spectra.

The dependence of the obtained quasielastic broadening, Γ, on the momentum transfer, Q, is displayed in figure 4 for the spectra at 110 and 120 K. Figure 4 also contains fits of the data to the theoretical models presented in section 3. The data clearly deviate from the pure parabola obtained by spin-echo spectroscopy at values of $Q > 1$ Å^{-1} and we can, thus, exclude a pure Brownian diffusion here. On the other hand we find that the Q range of the BS measurements is insufficient to decide between different jump diffusion models. Hence, it is adequate to use the model with the smallest number of fitting parameters, i.e., the Chudley–Elliott model, for extracting quantitative data. Table 1 displays the data that are extracted by applying the Chudley–Elliott model. We believe that a rotational jump diffusion can explain the high Q broadenings, since the extracted jump distances of about 2.1 Å correspond well to the distance between adjacent h-atoms on the benzene ring (2.48 Å [47, 48]).

We should stress that the backscattering measurements test energy broadenings in the μeV range, three orders of magnitude below the meV broadenings found with spin-echo. This indicates that the rotational diffusion observed here is a rather slow process. The Arrhenius energy barrier of $\bar{E}_a = 8.9 \pm 1.0$ meV that was found in this measurement, however, is very small and similar to the energy barrier found in the spin-echo translational collective diffusion studies (17 ± 12 meV). Contrary to the coherent scattering spin-echo data [8], it was also found that the molecules stay mobile below 110 K (see figure 5), a temperature at which only a static signal was found in the NSE experiments.

We see a possible explanation for the observed phenomena in the fact that benzene forms islands at low temperature, as observed in recent force-field MD simulations [21]. These islands could be immobilized by surface defects below a 2d freezing temperature. In these islands rotations of the benzene

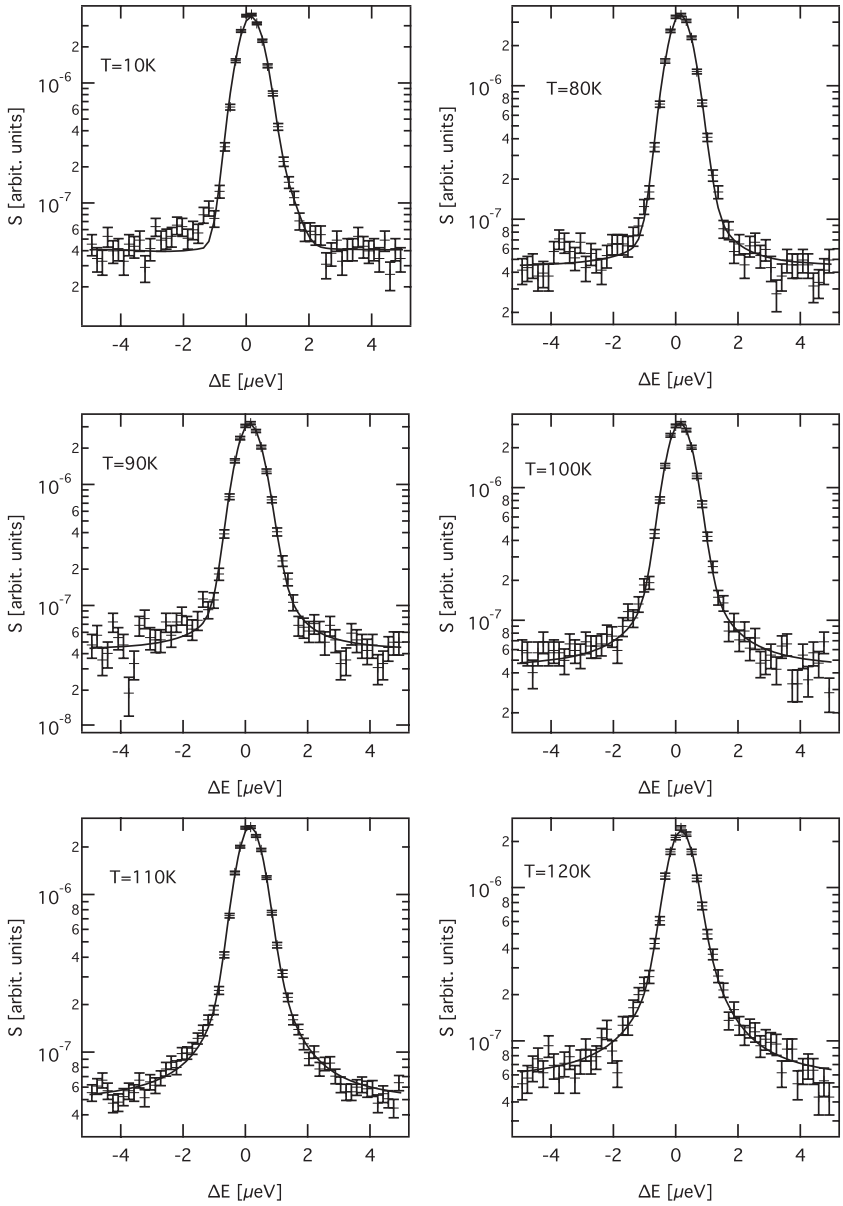

Figure 3. Backscattering spectra measured at different temperatures at a momentum transfer of $Q = 0.86$ Å^{-1}. The fits (solid lines) use a sum of a Gaussian and a Voigt function. The top-left data, measured at 10 K, represents a measurement of the resolution function and is fitted by a pure Gaussian function with a HWHM of 0.9 μeV.

'clock wheels' and/or translational diffusion would require site exchanges which are invisible in coherent scattering, but visible in incoherent scattering [49]. We would like to stress that the analysis of the self diffusion of benzene on graphite is not complete, and that the experimental Q ranges are insufficient for establishing a firm model of the exact diffusion mechanism. Further spectroscopic and theoretical studies are essentially needed.

6. Finite size effects and surface defects: incoherent and coherent scattering studies of benzene diffusion on carbon black

In the last sections we have seen that benzene is an excellent test system for studying surface diffusion phenomena displaying almost ideal Brownian long range diffusion. Thus, benzene–graphite should be an ideal system for studying how surface defects and boundaries influence diffusion. A wide range of techniques exist to manipulate graphitic systems today, and graphitic materials with different purity and surface size are available from commercial suppliers.

As a test for the feasibility of these studies we have performed exploratory NSE spectroscopy measurements on the IN11C spectrometer at ILL, using Vulcan XC-72 and Black Pearls 2000 (BP2000) carbon black powders as substrates.

In a first set of experiments we adsorbed 0.5 ML of deuterated benzene on both samples, leading to predominantly coherent scattering. For neither substrate did we find any dynamic NSE signal, i.e., no diffusion processes within the time and space scale tested by NSE. It is very likely

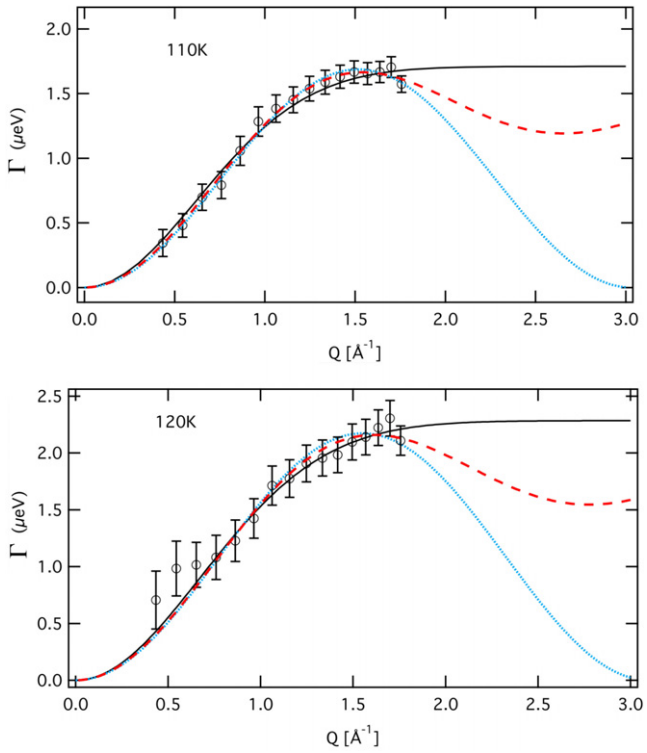

Figure 4. Comparison between theoretical functions based on the three considered models and the extracted quasielastic broadening at temperatures of 110 and 120 K. The black continuous line represents the Singwi–Sjolander model, the red dashed line is the isotropic Chudley–Elliott model and the blue dotted line is the Chudley–Elliott function. The open circles represent the quasielastic broadening extracted from the experimental data.

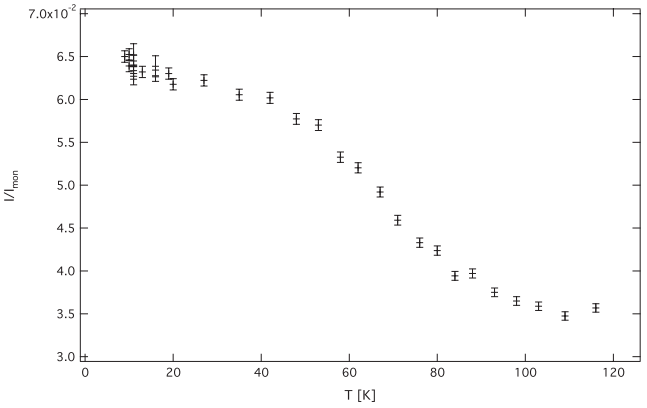

Figure 5. Fixed window (elastic) scan performed in the IN16 backscattering experiment, when cooling the system from 120 to 10 K. Due to the resolution used in this particular experiment, this scan shows the neutrons undergoing less than 0.9 μeV energy transfer. The data are integrated over the momentum transfer range 0.4 Å^{-1} $< Q <$ 1.7 Å^{-1}.

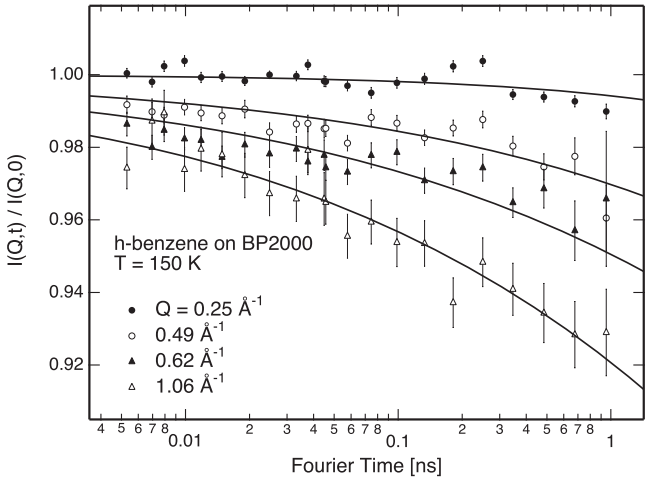

Figure 6. NSE spectra of an 0.5 ML film of h-benzene adsorbed on a BP2000 carbon black sample at a sample temperature of 150 K. The solid lines are KWW function fits using a stretching exponent, β of 0.3.

that the small dimensions, high defect density and/or the curved geometry of the graphite surfaces in these strongly fractured powders promoted island formation or pinning and, hence, prevented the observation of diffusion in coherent scattering. Here, we should remind the reader that coherent scattering does not distinguish between identical particles [49]. Site-exchange diffusion and jump rotation of a molecule with six-fold rotational symmetry cannot be observed. The average particle size of Vulcan XC-72 is 30 nm for primary particles and 370 nm for aggregate bunches in vacuum with a distribution of 250–500 nm [50, 51]. For BP2000, high-resolution transmission electron microscope (HRTEM) studies established an average particle diameter of 12 nm and a particle size distribution of 8–20 nm [52].

In a second set of experiments on the BP2000 substrate we adsorbed an 0.5 ML film of hydrogenated benzene. Here, we found a clear signature of diffusive dynamics (see figure 6). As could be expected intuitively—and contrary to the result of diffusion on exfoliated graphite (SE or BS)—we found no single rate of diffusion, but a wide distribution of diffusion rates. A distribution of diffusion rates leads to a widened decay curve that is often modelled by a stretched exponential decay function (or Kohlrausch Williams Watts function, KWW)

$$I(Q,t) = A + (1-A)\exp\left[-\left(\frac{t}{\tau}\right)^{\beta}\right], \qquad (14)$$

where A is the fraction of static signal and β is the stretching exponent ($\beta \leqslant 1$, with $\beta = 1$ for a single exponential decay). In the present spectra for BP2000 powders we found relaxation that could be fitted only by choosing $\beta \sim 0.4$, but due to the limited time and temperature range of this exploratory study we were not able to determine a precise value for β for different momentum transfers. The fits shown in figure 6 use an imposed value of $\beta = 0.3$ for all Q values, which represents the data rather well. The relaxation times are clearly Q dependent, but the data are not sufficient to determine the exact nature of the diffusion processes involved. At this moment it is unclear how much of the observed diffusional motion is caused by translational or rotational diffusion. A stretched exponential decay, however, is generally caused by a complex PES with varying activation barriers for different diffusion pathways. In the present case, we find that the stretched exponential covers relaxation rates from the short timescale observed with

spin-echo on exfoliated graphite to the long timescales that were observed in the BS study (1 ns corresponds to ∼4 μeV).

Further measurements using both spin-echo and time-of-flight spectroscopy on different energy/timescales are very much needed to characterize the motion. Spin-echo spectroscopy measurements will probably have to wait for the launch of the wide angle NSE spectrometer WASP at ILL [27, 28], whereas time-of-flight spectrometers such as IN5 at ILL have recently been enhanced sufficiently for the benzene/graphite studies [30]. For these studies a variety of different carbon blacks, active carbons and ordered nanoscale carbons, such as nanotubes, are available.

7. Computational modelling of surface diffusion of cyclic hydrocarbons on graphite

Computational modelling has been essential for correctly interpreting a large part of recent quasielastic spectroscopic data [4] (the results of real diffusion measurements are rarely fully described by the models presented in section 3). In addition, theoretical modelling is a rich source of ideas for new avenues of surface diffusion research. In this section we will give a short overview of the methods and recent results, with an emphasis on open questions that could be approached by spectroscopic studies.

Much effort has been devoted to the theoretical modelling of diffusion [24, 53–65] and friction [66–69] processes on surfaces. Due to space restrictions in this paper, the references given above represent only a fraction of recent work, with an emphasis on general theoretical models and calculations applied to benzene and graphitic systems.

In general, we can distinguish two major approaches to the simulation of surface diffusion: firstly, it is possible to understand the generic properties of different diffusion processes by transition state theory or by applying the Langevin equation. Secondly, diffusion or friction dynamics can be studied by applying force-field molecular dynamics (MD). The latter approach is mainly used if the bonding between the molecules and the surface is weak, i.e. if the molecules are physisorbed.

In the Langevin equation approach, the Langevin equation of motion

$$m\frac{\mathrm{d}\vec{v}_\mathrm{i}}{\mathrm{d}t} = -\nabla U - \eta m\vec{v}_\mathrm{i} + \sum_{j\neq i}\vec{F}_{i,j} + \zeta(t) \qquad (15)$$

is used to study the trajectories of molecules moving on a surface, typically reduced to two dimensions, where m is the mass of the molecules, $\vec{v}_\mathrm{i}$ is the velocity of the ith molecule, t is the time, U is the potential energy for the molecule on the surface, η is the frictional coupling of the molecule to the surface, $\vec{F}_{i,j}$ is the force between molecule i and j, and finally, ζ gives random impulses on the molecules, which are determined from the friction by the fluctuation-dissipation theorem [70]. The Langevin equation can be used to find the generic response of a system to given parameters by testing, for example, how a system responds to low or high friction for a given potential energy surface geometry. This approach is the tool of choice for exploring phase space for new physical phenomena. Recently, effects such as superdiffusion, nonlinear dynamics, chaos, and the influence of quantum effects have been investigated [24, 58–60, 64, 65, 71, 72].

The Langevin method can also be used to extract data such as the diffusion barrier or the Einstein friction parameter from experimental data by 'fitting' parameters, such as the interaction potential U and the friction parameter η, to achieve simulation results that best coincide with experimental spectra. This approach has been applied successfully in recent work on helium time-of-flight and spin-echo spectroscopy [8, 73–77]. Furthermore, the Langevin equation approach can be used to compare experimental studies with density functional theory (DFT) studies. In this case, the PES derived using DFT can be used as an input to the Langevin equation (15) and only the friction is left as a free parameter for fitting. The DFT approach is particularly useful for the study of molecules that are chemisorbed to the surface, such as, e.g., CO and NO on metal surfaces. In these cases, the diffusion barriers are in the range of $\geqslant$100 meV, such that DFT can give sufficient accuracy with a typical error bar for the barrier height of about 10–20 meV [78, 79].

The force-field MD method, which we describe in the following, is theoretically quite similar to the Langevin method. Here, the equation of motion can be written as:

$$m\frac{\mathrm{d}\vec{v}_\mathrm{i}}{\mathrm{d}t} = \sum_{j\neq i\neq k}\nabla U_{i,j,k}(\vec{r}_{i,j}, \vec{r}_{i,k}, \theta_{j,i,k}), \qquad (16)$$

where $U_{i,j,k}$ is the potential energy of atom i with respect to its neighbours j and k. The sum runs over all atoms within a given radius. The force-field MD equation of motion (16) is strongly simplified with respect to the Langevin equation (15) as no friction or impulse term is used. On the other hand, Langevin equation simulations typically use only a simple two dimensional periodic PES, whereas the potential energy U in force-field MD is calculated between all atoms within a given range. For atoms connected by chemical bonds there can be a high number of terms, including bond stretching and bending terms (represented in the formula by the vectors for the bond distances $\vec{r}_{i,j}$ and $\vec{r}_{i,k}$ and the bending angle $\theta_{j,i,k}$) as well as their higher order mixing terms. The accuracy of these terms is crucial for the correct simulation of phonons and energy dissipation in the system. However, the interaction between the diffusing molecules and the surface cannot be modelled with these terms as they foresee no bond breaking and, thus, only so-called non-bonding terms are used, i.e. electrostatic and van der Waals interaction. Therefore, this method is only suited for the study of physisorbed molecules and the force-field MD method is most widely used for the study of molecule adsorption on surfaces such as graphite [21, 53–55, 57]. The force-field MD calculations cannot be used to extract quantities such as the friction parameter directly, however they allow one to establish a PES guiding the diffusion and they allow one to predict diffusion properties of molecules on surfaces if no measurements are available and if the force-field has been validated by experiments for similar systems. In particular, the latter point opens the possibility of technological applications

of the data extracted from neutron and helium spectroscopic data.

One of the important open questions in surface diffusion deals with the role of chaos and non-linearity in surface diffusion and its appropriate description. Non-linearity and, thus, chaotic dynamics can be introduced, not only by interaction with the environment (external noise), but by the interactions between molecules and surfaces if a sufficient number of degrees of freedom exist [80]. (Poly-)cyclic hydrocarbons are candidates for the observation of this phenomenon, since rotation and translational motion should interfere and have sufficiently different activation energies. Force-field MD simulations have been applied successfully to the benzene/graphite diffusion [21] and have allowed the study of a range of phenomena such as the link between rotational and translational motion as well as a potential contribution of anomalous transport [21]. Anomalous transport is, in general terms, any deviation from Brownian long range diffusion. It is normally described by a generalized Einstein equation of motion of the following form:

$$\langle |\mathbf{R}(t) - \mathbf{R}(0)|^2 \rangle \propto D_\alpha t^\alpha, \tag{17}$$

where $\langle |\mathbf{R}(t) - \mathbf{R}(0)|^2 \rangle$ is the mean square displacement and $\alpha < 1$ (subdiffusion) or $\alpha > 1$ (enhanced diffusion or superdiffusion) describes diffusion processes that are slower or faster than ordinary Brownian motion. Many recent theoretical studies have been devoted to anomalous diffusion behaviour on surfaces (e.g. [71, 81]), but experimental evidence for this phenomenon has not yet been found. For benzene on graphite diffusion, α was found to be 1, i.e., the diffusion was not anomalous. Closely linked future theoretical and experimental research into the diffusion of cyclic hydrocarbons on graphitic surfaces, however, promises to help realizing an experimental example using graphene flakes or larger hydrocarbon molecules.

Finally, the theoretical diffusion models that are newly developed and/or validated can be used to lay a base for the application of graphitic materials in nanomechanics and nanoelectronics. Carbon has mechanical and electronic properties that make it one of the most widely studied materials for these applications [9, 82]. Evidently, a deep understanding of the microscopic interactions between carbon containing systems is essential for the construction of carbon nanomachines. Recent force-field MD calculations, which were based on the widely used forcefields COMPASS, Dreiding and Universal, have allowed the establishment of a relation between static and dynamic friction by linking a PES that delivers an excellent description of spectroscopic data [21] (see figure 7) to a PES that was extracted from friction force microscopy (FFM) [67]. The diffusion PES was established by calculating the energy of the adsorbed molecule at representative positions on the surface, taking into account only the (non-bonding) electrostatic and van der Waals terms. We consider this as a promising first step in spectroscopic studies of nanomechanical carbon entities.

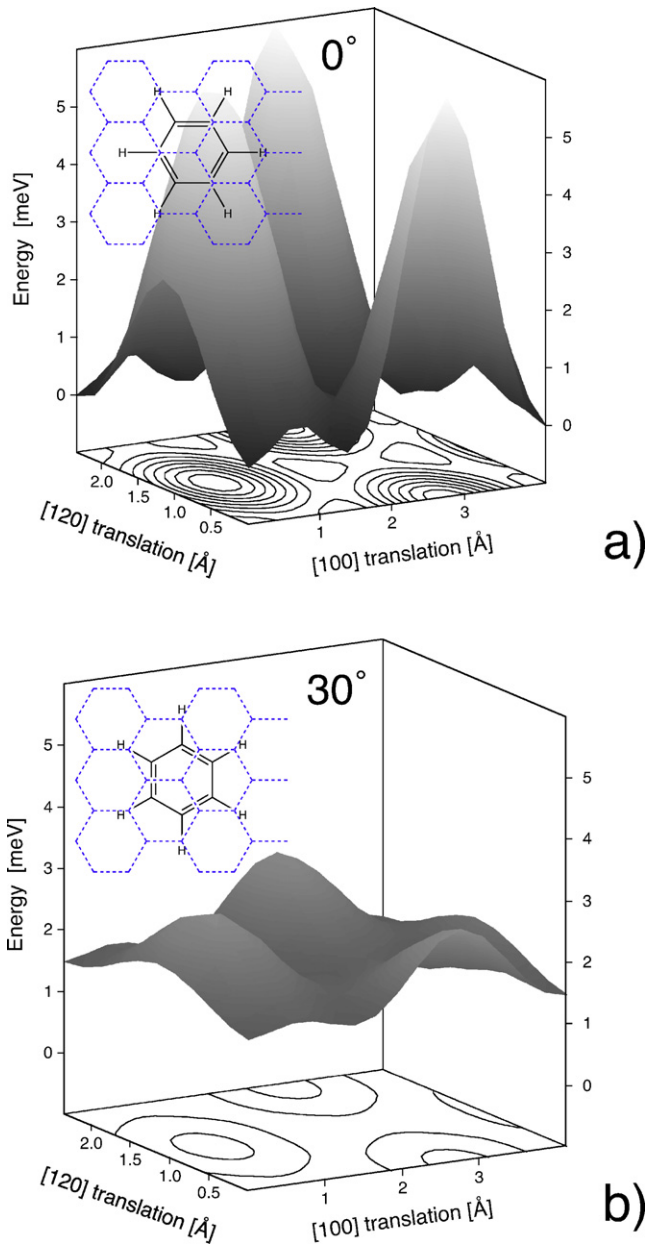

Figure 7. Potential energy surfaces (PES) for the translation of benzene molecules adsorbed flat on graphite in two different rotational orientations. The PES are based on the COMPASS force-field [21]. The PES is strongly flattened, when the molecules are rotated out of alignment with the graphite structure (graph b). The flattening of the PES upon rotation of the molecules was termed superlubrication in SPM studies [15].

8. Conclusions and open questions

In the preceding paragraphs, we have reviewed the methodology and results of recent research into diffusion and friction of benzene molecules on graphite surfaces. A large part of the presented material is work in progress and further studies will be needed to get a final picture of the observed phenomena. The synopsis of the data, however, delivers a number of clues for the interpretation and motivation for future research.

Earlier studies of benzene adsorbed on basal plane graphite have revealed adsorption energies [83], struc-

ture [36, 37, 84] and some information about rotation and diffusion behaviour [48, 85–90]. For a long time it was unclear if the benzene molecules adsorb flat on the surface (molecular plane parallel to the substrate surface) or if a substantial fraction of molecules remains in a tilted orientation. Molecular dynamics (MD) calculations were performed to resolve the issue [53–55, 57], but only a review of earlier NMR measurements gave final evidence that benzene adsorbs almost predominantly flat on graphite at sub-monolayer coverages below the monolayer desorption temperature of 150 K [89]. Sub-monolayers are now agreed to adsorb flat, but at coverages of more than 1 ML a large fraction of the molecules adsorb strongly tilted.

The *long range diffusion* of sub-monolayer benzene on basal plane graphite, which was studied with spin-echo spectroscopy under *coherent scattering* conditions, gives a remarkable example of pure Brownian motion down to a very small length scale of about 4 Å (section 5). It would be very interesting to see to which length scale the Brownian law is conserved. Such a study should be performed using a neutron spin-echo spectrometer, which allows measurements at momentum transfers on the order of 3 $Å^{-1}$ (such as SPAN at HZB, Berlin).

Exploratory *incoherent scattering* studies of benzene diffusion on basal plane graphite on high-resolution neutron backscattering spectrometers display characteristics of jump diffusion. This has been tentatively attributed to a rotational jump diffusion, as the jump distance given by the Chudley–Elliott model is similar to the distance between the hydrogen atoms on the benzene ring. Further incoherent scattering studies should cover larger Q ranges and as large an energy scale as possible to reveal the nature of the measured diffusion and to establish the interaction between translational and rotational motion. These studies would require the use of spectrometers at high flux sources, due to the low surface signal, and the use of a range of instruments to cover the required spectroscopic range.

Both scattering studies, coherent and incoherent, should be extended towards larger aromatic molecules, such as naphthalene, coronene, and ovalene, because present experimental and theoretical evidence hints towards a similar excitation energy for rotation and translation, and to a coupling between these degrees of freedom, which would ultimately allow the study of non-linearity in these systems (see section 7). For large graphene sheets adsorbed on graphite (comparable in size to ovalene molecules) friction force microscopy measurements and related calculations have demonstrated a process that was termed 'superlubrication': if these molecules are brought into an orientation which is out of phase with the graphite substrate, they can be moved with negligible friction. This effect is linked to the perfect Brownian diffusion of benzene on graphite, in our view, and it would be very interesting to study this in more detail for larger aromatic molecules. It is interesting to note that in this case a very low static friction is observed together with rather high dynamic friction. The low static friction prevents translational jump diffusion, but the surface layer of the graphite is phononically so soft that the benzene molecules can efficiently exchange energy with the substrate, which leads to a high dynamic friction. This interpretation is supported by the very soft graphite multiphonon feature that was observed in the HeSE measurements [46]. Potential differences between the surface interaction of aromatic hydrocarbons and graphene molecules should also be studied.

With benzene/graphite being an almost perfectly diffusing system, benzene/graphite should be used to study finite size effects of surfaces and confinement effects. In section 6 we have demonstrated that no diffusion signal is obtained in carbon blacks under coherent scattering conditions, but that it is possible to observe self diffusion and rotational diffusion. We have observed a wide distribution of diffusion rates, which we believe to be caused by the wide distribution of the size of graphite/graphene surfaces in these samples. These studies should be continued for a range of carbon blacks and active carbons to create a solid basis for MD models of the influence of finite surface size and boundaries on molecular mobility. These models would, in a second step, give essential information towards the understanding of finite size and surface interaction effects in studies of molecules confined in carbon channels (see for example [91]). The dynamics of liquids in confinement differ substantially from bulk liquids, and the changes in the thermodynamic properties allow, for example, the study of strongly undercooled liquids. A major contribution to this field of research is possible if the surface dynamics of a larger group of (small) molecules are understood. Thus, future research should include molecules such as cyclohexane, toluene, and—last but not least—water.

A substantial progress in the understanding of surface diffusion and friction processes hinges on the quality of the theoretical models and on the availability of detailed simulations of the observed spectra. We have shown that considerable advances have been achieved in the description of aromatic hydrocarbons on graphite, but we believe that there is a large potential for further developments. It is certainly beneficial for this topic that much attention has been drawn recently to a very similar system, graphene. Modern forcefields are capable of giving an excellent description of benzene/graphite dynamics, and they could be used to study non-linearity phenomena as well as nanomechanical applications of aromatic hydrocarbons.

Acknowledgments

The authors are grateful to G Alexandrowicz, W Allison, J Ellis, H Hedgeland, A P Jardine, M R Johnson, J Z Larese, and S Miret-Artés for the many stimulating discussions. Cabot Corp. is gratefully acknowledged for providing the carbon black samples.

References

[1] Bruch L W, Diehl R D and Venables J A 2007 *Rev. Mod. Phys.* **79** 1381–454
[2] Jardine A P, Hedgeland H, Alexandrowicz G, Allison W and Ellis J 2009 *Prog. Surf. Sci.* **84** 323–79
[3] Brune H 2009 *Ann. Phys.* **18** 675–98

[4] Fouquet P, Hedgeland H and Jardine A P 2010 *Z. Phys. Chem.* **224** 61–81
[5] Jardine A P, Dworski S, Fouquet P, Alexandrowicz G, Riley D J, Lee G Y H, Ellis J and Allison W 2004 *Science* **304** 1790–3
[6] Kärger J, Valiullin R and Vasenkov S 2005 *New J. Phys.* **7** 15
[7] Backus E H G, Eichler A, Kleyn A W and Bonn M 2005 *Science* **310** 1790–3
[8] Hedgeland H, Fouquet P, Jardine A P, Alexandrowicz G, Allison W and Ellis J 2009 *Nat. Phys.* **5** 561–4
[9] Bhushan B (ed) 2005 *Nanotribology and Nanomechanics—An Introduction* (Berlin: Springer)
[10] Heinrich A J, Lutz C P, Gupta J A and Eigler D M 2002 *Science* **298** 1381–7
[11] Miura K and Kamiya S 2002 *Europhys. Lett.* **58** 610–5
[12] Miura K, Kamiya S and Sasaki N 2003 *Phys. Rev. Lett.* **90** 055509
[13] Stroscio J A and Celotta R J 2004 *Science* **306** 242–7
[14] Socoliuc A, Bennewitz R, Gnecco E and Meyer E 2004 *Phys. Rev. Lett.* **92** 134301
[15] Dienwiebel M, Verhoeven G S, Pradeep N, Frenken J W M, Heimberg J A and Zandbergen H W 2004 *Phys. Rev. Lett.* **92** 126101
[16] Park J Y, Ogletree D F, Thiel P A and Salmeron M 2006 *Science* **313** 186
[17] Frenken J 2006 *Nat. Nanotechnol.* **1** 20–1
[18] Cannara R J, Brukman M J, Cimatu K, Sumant A V, Baldelli S and Carpick R W 2007 *Science* **318** 780–3
[19] Ternes M, Lutz C P, Hirjibehedin C F, Giessibl F J and Heinrich A J 2008 *Science* **319** 1066–9
[20] Albers B J, Schwendemann T C, Baykara M Z, Pilet N, Liebmann M, Altmann E I and Schwarz U D 2009 *Nat. Nanotechnol.* **4** 307–10
[21] Fouquet P, Johnson M R, Hedgeland H, Jardine A P, Ellis J and Allison W 2009 *Carbon* **47** 2627–39
[22] Gomer R 1990 *Rep. Prog. Phys.* **53** 917–1002
[23] Barth J V 2000 *Surf. Sci. Rep.* **40** 75–149
[24] Ala-Nissila T, Ferrando R and Ying S C 2002 *Adv. Phys.* **51** 949–1078
[25] Naumovets A G 2005 *Physica* A **357** 189–215
[26] Farago B 1999 *Physica* B **268** 270–6
[27] Fouquet P, Ehlers G, Farago B, Pappas C and Mezei F 2007 *J. Neutron Res.* **15** 39–47
[28] Fouquet P, Farago B, Andersen K H, Bentley P M, Pastrello G, Sutton I, Thaveron E, Thomas F, Moskvin E and Pappas C 2009 *Rev. Sci. Instrum.* **80** 095105
[29] Jardine A P, Alexandrowicz G, Hedgeland H, Allison W and Ellis J 2009 *Phys. Chem. Chem. Phys.* **11** 3355–74
[30] ILL 2008 *The Yellow Book 2008* (Grenoble: Institut Laue Langevin)
[31] Mezei F (ed) 1980 *Neutron Spin Echo* (*Lecture Notes in Physics* vol 128) (Berlin: Springer)
[32] Gähler R, Golub R, Habicht K, Keller T and Felber J 1996 *Physica* B **229** 1–17
[33] van Hove L 1954 *Phys. Rev.* **95** 249–62
[34] Bée M 1988 *Quasielastic Neutron Scattering* (Bristol, PA: Adam Hilger)
[35] Frick B, Mamontov E, van Eijck L and Seydel T 2010 *Z. Phys. Chem.* **224** 33–60
[36] Bardi U, Magnanelli S and Rovida G 1985 *Surf. Sci. Lett.* **165** L7–11
[37] Gameson I and Payment T 1986 *Chem. Phys. Lett.* **123** 150–3
[38] Hempelmann R 2000 *Quasielastic Neutron Scattering and Solid State Diffusion* (Oxford: Oxford University Press)
[39] Ross D K, Kemali M and Bull D J 1999 *Anomalous Diffusion: from Basics to Applications* (*Lecture Notes in Physics* vol 519) ed A Pekalski and K Sznajd-Weron (Berlin: Springer) pp 45–60
[40] Vineyard G H 1958 *Phys. Rev.* **110** 999–1010
[41] Ellis J, Graham A P and Toennies J P 1999 *Phys. Rev. Lett.* **82** 5072–5
[42] Einstein A 1905 *Ann. Phys.* **17** 549–60
[43] Chudley C T and Elliott R J 1961 *Proc. Phys. Soc. Lond.* **77** 353–61
[44] Singwi K S and Sjolander A 1960 *Phys. Rev.* **119** 863–71
[45] Fouquet P, Hedgeland H, Jardine A P, Alexandrowicz G, Allison W and Ellis J 2006 *Physica* B **385** 269–71
[46] Hedgeland H 2006 The development of quasi-elastic helium-3 spin-echo spectroscopy as a tool for the study of surface dynamics *PhD Thesis* University of Cambridge
[47] Pauling L 1960 *The Nature of the Chemical Bond* (Ithaca, NY: Cornell University Press)
[48] Stockmeyer R and Stortnik H 1979 *Surf. Sci.* **81** L315–8
[49] Coddens G 2001 *Phys. Rev.* B **63** 064105
[50] Claguea A D H, Donnetb J B, Wangb T K and Pengb J 1999 *Carbon* **37** 1553–65
[51] Bang J H, Han K, Skrabalak S E, Kim H and Suslick K S 2007 *J. Phys. Chem.* C **111** 10959–64
[52] Zhu W, Miser D E, Chan W G and Hajaligol M R 2004 *Carbon* **42** 1841–5
[53] Clifton B and Cosgrove T 1998 *Mol. Phys.* **93** 767–76
[54] Vernov A and Steele W A 1991 *Langmuir* **7** 2817–20
[55] Vernov A and Steele W A 1991 *Langmuir* **7** 3110–7
[56] Chen L Y, Baldan M R and Ying S C 1996 *Phys. Rev.* B **54** 8856–61
[57] Matties M A and Hentschke R 1996 *Langmuir* **12** 2501–4
[58] Shushin A I and Pollak E 2003 *J. Chem. Phys.* **119** 10941–52
[59] Sancho J M, Lacasta A M, Lindenberg K, Sokolov I M and Romero A H 2004 *Phys. Rev. Lett.* **92** 250601
[60] Miret-Artés S and Pollak E 2005 *J. Phys.: Condens. Matter* **17** S4133–50
[61] Lindenberg K, Lacasta A M, Sancho J M and Romero A H 2005 *Unsolved Problems of Noise and Fluctuations: UPoN 2005* vol CP800, ed L Reggiani, C Pennetta, V Akimov, E Alfinito and M Rosini (New York: AIP) pp 50–5
[62] Martínez-Casado R, Vega J L, Sanz A S and Miret-Artés S 2007 *J. Chem. Phys.* **126** 194711
[63] Martínez-Casado R, Vega J L, Sanz A S and Miret-Artés S 2007 *Phys. Rev. Lett.* **98** 216102
[64] Martínez-Casado R, Vega J L, Sanz A S and Miret-Artés S 2008 *Phys. Rev.* B **77** 115414
[65] Martínez-Casado R, Sanz A S and Miret-Artés S 2008 *J. Chem. Phys.* **129** 184704
[66] Ringlein J and Robbins M O 2004 *Am. J. Phys.* **72** 884–91
[67] Verhoeven G S, Dienwiebel M and Frenken J W M 2004 *Phys. Rev.* B **70** 165418
[68] Jinesh K B, Krylov S Y, Valk H, Dienwiebel M and Frenken J W M 2008 *Phys. Rev.* B **78** 155440
[69] Mo Y, Turner K T and Szlufarska I 2009 *Nature* **457** 1116–9
[70] Kubo R 1966 *Rep. Prog. Phys.* **29** 255–84
[71] Guantes R, Vega J L and Miret-Artés S 2001 *Phys. Rev.* B **64** 245415
[72] Martínez-Casado R, Vega J L, Sanz A S and Miret-Artés S 2007 *J. Phys.: Condens. Matter* **19** 305002
[73] Jardine A P, Ellis J and Allison W 2002 *J. Phys.: Condens. Matter* **14** 6173–91
[74] Alexandrowicz G, Jardine A, Fouquet P, Dworski S, Allison W and Ellis J 2004 *Phys. Rev. Lett.* **93** 156103
[75] Alexandrowicz G, Jardine A P, Hedgeland H, Allison W and Ellis J 2006 *Phys. Rev. Lett.* **97** 156103
[76] Jardine A P, Alexandrowicz G, Hedgeland H, Diehl R D, Allison W and Ellis J 2007 *J. Phys.: Condens. Matter* **19** 305010
[77] Alexandrowicz G, Kole P, Lee E, Hedgeland H, Ferrando R, Jardine A, Allison W and Ellis J 2008 *J. Am. Chem. Soc.* **130** 6789–94
[78] Feibelmann P J, Hammer B, Norskov J K, Wagner F, Scheffler M, Stumpf R, Watwe R and Dumesic J 2001 *J. Phys. Chem.* B **105** 4018–25

[79] Fouquet P, Olsen R A and Baerends E J 2003 *J. Chem. Phys.* **119** 509–14
[80] Lichtenberg A J and Lieberman M A 1992 *Regular and Chaotic Dynamics* (New York: Springer)
[81] Vega J L, Guantes R and Miret-Artés S 2002 *J. Phys.: Condens. Matter* **14** 6193–232
[82] Dumitrica T (ed) 2010 *Trends in Computational Nanomechanics—Transcending Length and Time Scales* (*Challenges and Advances in Computational Chemistry and Physics* vol 9) (Berlin: Springer)
[83] Zacharia R, Ulbricht H and Hertel T 2004 *Phys. Rev.* B **69** 155406
[84] Bardi U, Magnanelli S and Rovida G 1987 *Langmuir* **3** 159–63
[85] Boddenberg B and Moreno J A 1976 *Z. Naturf.* a **31** 853–4
[86] Boddenberg B and Moreno J A 1977 *J. Phys. Colloq.* **38** C4 52–5
[87] Monkenbusch M and Stockmeyer R 1980 *Ber. Bunsenges. Phys. Chem.* **84** 808–14
[88] Tabony J, White J W, Delachaume J C and Coulon M 1980 *Surf. Sci.* **95** L282–8
[89] Boddenberg B and Grosse R 1986 *Z. Naturf.* a **41** 1361–8
[90] Grosse R and Boddenberg B 1987 *Z. Phys. Chem.* **152** 1–12
[91] Frick B, Alba-Simionesco C, Dosseh G, Le Quellec C, Moreno A J, Colmenero J, Schonhals A, Zorn R, Chrissopoulou K, Anastasiadis S H and Dalnoki-Veress K 2005 *J. Non-Cryst. Solids* **351** 2657–67